



ELSEVIER

Contents lists available at ScienceDirect

## Journal of Magnetism and Magnetic Materials

journal homepage: [www.elsevier.com/locate/jmmm](http://www.elsevier.com/locate/jmmm)

## Effect of Co addition on the magnetic properties and microstructure of FeNbCu nanocrystalline alloys

Lin Xue<sup>a,b,c</sup>, Weiming Yang<sup>c</sup>, Haishun Liu<sup>c,\*</sup>, He Men<sup>b</sup>, Anding Wang<sup>b,\*</sup>, Chuntao Chang<sup>b</sup>, Baolong Shen<sup>a,\*</sup><sup>a</sup> School of Materials Science and Engineering, Southeast University, Nanjing 211189, China<sup>b</sup> Ningbo Institute of Industrial Technology, Chinese Academy of Sciences, Ningbo 315201, China<sup>c</sup> School of Sciences, China University of Mining and Technology, Xuzhou 221116, China

## ARTICLE INFO

## Article history:

Received 23 September 2015

Received in revised form

3 June 2016

Accepted 9 June 2016

Available online 16 June 2016

## Keywords:

Nanocrystalline alloys

High saturation magnetization

Grain size

## ABSTRACT

Through gradient substitution of Co for Fe, the magnetic properties and microstructures of  $(\text{Fe}_{1-x}\text{Co}_x)_{83}\text{Nb}_2\text{B}_{14}\text{Cu}_1$  ( $x=0.1, 0.2, 0.3, 0.4, 0.5$ ) nanocrystalline alloys were investigated. Because of the strong ferromagnetic exchange coupling between Co and Fe, substantial improvement in saturation magnetization was achieved with proper levels of Co addition. Meanwhile, the Curie temperature increased noticeably with increasing Co addition. After heat treatment, the  $(\text{Fe}_{0.9}\text{Co}_{0.1})_{83}\text{Nb}_2\text{B}_{14}\text{Cu}_1$  nanocrystalline alloy showed a refined microstructure with an average grain size of 10–20 nm, exhibiting a comparatively high saturation magnetization of 1.82 T and a lower coercivity of 12 A/m compared to other Hitperm-type alloys with higher Co contents. Additionally, the Curie temperature reached 1150 K upon introduction of Co. As the soft magnetic properties are strengthened by adding a small amount of Co, the combination of fine, soft magnetic properties and low cost make this nanocrystalline alloy a potential magnetic material.

© 2016 Elsevier B.V. All rights reserved.

## 1. Introduction

Since the ferromagnetic Fe–P–C amorphous alloy was synthesized for the first time in 1967 [1], Fe- and (Fe, Co)-based alloys have constituted an important category of soft magnetic materials with a wide and important range of technological applications where high magnetic flux densities are required. To date, these materials have found application in data storage, high-performance transformers, and pole tips for high-field magnets [2–4]. Together with their high strength and good corrosion resistance, ferromagnetic amorphous alloys may have a promising future in applications such as advanced functional and structural materials [5–8]. Additionally, most of the nanocrystalline soft magnetic systems are composed of a special nanometer duplex structure wherein randomly oriented nanoparticles with an average size from several to several tens of nanometers are dispersed in an amorphous matrix, resulting in nanocrystalline alloys exhibiting excellent soft magnetic properties [9]. These soft magnetic properties, especially the extrinsic properties such as magnetic permeability and coercivity, could be strongly affected by structural

and compositional variation [10–12]. To date, the combination of superior soft magnetic properties, high saturation magnetization and, in particular, low cost have fueled the interest in Fe-based nanocrystalline materials. Subsequently, Finemet, which has excellent comprehensive soft magnetic properties [13], and Nanoperm, with its high saturation magnetization, were developed [14]. Because higher saturation magnetization makes the devices smaller and lighter and a high Curie temperature was necessary in high temperature environments, Hitperm was developed with high saturation magnetization and a high Curie temperature by introducing Co in Nanoperm [15]. Except for increasing the Fe content, Co-doping has been surmised to be an effective method for improving the saturation magnetization of many Fe-based alloys [16–18]. In addition, a magnetocaloric response was discovered in Fe-based alloys [19–21], and further, it was found that Co-containing Fe(Co)–M–B–Cu alloys exhibit noticeably larger magnetocaloric effects [21–23]. This performance expands the application range of FeCo-based alloys to a certain degree, making these ingredients a promising functional material. Therefore, it is important to study the influence of Co substitution on the magnetic properties and microstructures of Fe-based alloys.

Previously,  $\text{Fe}_{83}\text{Nb}_2\text{B}_{14}\text{Cu}_1$  nanocrystalline alloys with high saturation magnetization and low cost were developed [24]. It was found that the average grain size first increases and then decreases to a minimum between the crystallization temperatures, where

\* Corresponding authors.

E-mail addresses: [liuhaishun@126.com](mailto:liuhaishun@126.com) (H. Liu), [anding@nimte.ac.cn](mailto:anding@nimte.ac.cn) (A. Wang), [blshen@seu.edu.cn](mailto:blshen@seu.edu.cn) (B. Shen).

the optimal microstructure appears. Finally, the grain size increases again with increasing annealing temperatures for FeNbBCu nanocrystalline alloys, which results in undulating changes in coercivity and permeability. In the current work, to further improve the saturation magnetization and to investigate whether Co addition will influence the grain size variability of the base alloy, Fe was partially substituted by Co, and the soft magnetic properties of  $(\text{Fe}_{1-x}\text{Co}_x)_{83}\text{Nb}_2\text{B}_{14}\text{Cu}_1$  ( $x=0.1, 0.2, 0.3, 0.4, 0.5$ ) were studied. Furthermore, the sample that exhibited optimal magnetic properties was confirmed by investigating the corresponding microstructure. Using this information, we hope to gain insight into the microstructure of this material and achieve FeCoNbBCu compositions with better comprehensive properties.

## 2. Materials and methods

Fe-based alloy ingots with nominal compositions of  $(\text{Fe}_{1-x}\text{Co}_x)_{83}\text{Nb}_2\text{B}_{14}\text{Cu}_1$  ( $x=0.1, 0.2, 0.3, 0.4, 0.5$ ) were prepared by arc melting a mixture of pure Fe (99.99%), Co (99.99%), Nb (99.99%), B (99.5%), and Cu (99.99%) under a highly pure argon atmosphere. Ribbons with a width of approximately 1 mm and a thickness of approximately 20–25  $\mu\text{m}$  were produced by the single-roller melt spinning method. The crystallization temperature ( $T_x$ ) of as-quenched ribbons was measured by differential scanning calorimetry (DSC, NETZSCH 404C) with a heating rate of 0.67 K/s. Crystallization treatment was carried out by treating the as-quenched amorphous specimens at different temperatures for 180 s under vacuum, followed by water quenching. Microstructure was examined by X-ray diffraction (XRD, Bruker D8 Advance) with Cu  $K\alpha$  radiation ( $2\theta=20\text{--}90^\circ$ ) and transmission electronic microscopy (TEM, TECNAI F20). Saturation magnetic flux density ( $B_s$ ) and coercivity ( $H_c$ ) were measured using a vibrating sample magnetometer (VSM, Lake Shore 7410) under an applied field of 800 kA/m and a DC  $B$ - $H$  loop tracer (RIKEN BHS-40) under an applied field of 2 kA/m, respectively. The initial permeability ( $\mu_i$ ) in the frequency range of 1–101 kHz was measured with a vector impedance analyzer (Agilent 4294A) under a field of 1 A/m.

## 3. Results and discussion

Figs. 1 and 2 depict the characteristic microstructure and DSC curves of the as-quenched  $(\text{Fe}_{1-x}\text{Co}_x)_{83}\text{Nb}_2\text{B}_{14}\text{Cu}_1$  ( $x=0.1, 0.2, 0.3, 0.4, 0.5$ ) alloys. The XRD and DSC analyses conducted on the alloys yielded the following results. The diffraction peaks in Fig. 1 represent the fully amorphous phase, except for the alloys with  $x=0.5$ . The DSC curves show that the crystallization of all of these ribbons proceeds in two stages. A decrease of initial crystallization temperature ( $T_{x1}$ ) and an increase of second crystallization temperature ( $T_{x2}$ ) with an increase in Co content can also be observed. Therefore, the temperature interval ( $\Delta T_x=T_{x2}-T_{x1}$ ) between the two crystallization temperatures was enlarged, which is beneficial for crystallization heat treatment. The Curie temperature ( $T_c$ ) increases as the Co content increases, which indicates that Co substitution seems to enhance the thermal stability of the alloy matrix to a certain extent and increases the  $T_c$  at the same time.

The saturation magnetization of  $(\text{Fe}_{1-x}\text{Co}_x)_{83}\text{Nb}_2\text{B}_{14}\text{Cu}_1$  ( $x=0\text{--}0.4$ ) nanocrystalline alloys annealed for 180 s at varying annealing temperatures is shown in Fig. 3. It can be seen that the saturation magnetization under an applied field of 800 kA/m ( $B_{800}$ ) clearly increases from less than 1.4 T to higher than 1.6 T with the ferromagnetic element Co added to the as-quenched state, which can be attributed to the strong ferromagnetic exchange coupling between Co and Fe. The additions of Co could lead to alignment of the Fe moments and thereby increase the atomic magnetic

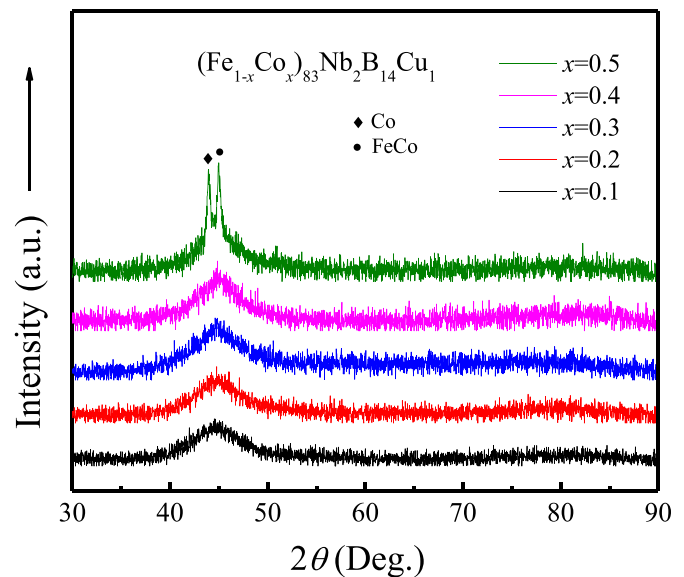


Fig. 1. XRD patterns of as-quenched  $(\text{Fe}_{1-x}\text{Co}_x)_{83}\text{Nb}_2\text{B}_{14}\text{Cu}_1$  alloys.

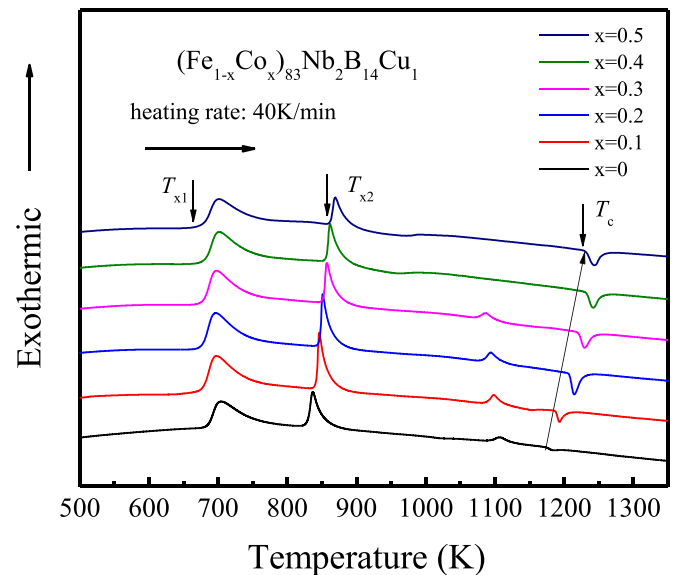


Fig. 2. DSC curves of as-quenched  $(\text{Fe}_{1-x}\text{Co}_x)_{83}\text{Nb}_2\text{B}_{14}\text{Cu}_1$  alloys.

moment of individual Fe atoms [25]. The  $B_{800}$  values of all alloys increase further with increasing annealing temperature ( $T_a$ ), which is caused by the appearance and growth of ferromagnetic crystalline grains embedded in the residual amorphous matrix and the increasing volume fraction of the nanocrystalline phase. Crystalline phases were identified as  $\alpha$ -(Fe, Co) for Co-added alloys and  $\alpha$ -Fe for alloys without Co by XRD, which indicates that the  $B_{800}$  of Co-containing alloys is higher than that of the base alloy.

Fig. 4 shows the  $H_c$  and  $\mu_i$  of  $(\text{Fe}_{1-x}\text{Co}_x)_{83}\text{Nb}_2\text{B}_{14}\text{Cu}_1$  ( $x=0\text{--}0.4$ ) nanocrystalline alloys annealed for 180 s versus those of alloys annealed at different temperatures. Compared to the base alloy, it shows that Co addition has no influence on the variation tendency of  $H_c$  and  $\mu_i$  as a function of temperature. However, it can be seen that the optimal annealing temperature increases and the temperature intervals become broader with Co addition, which is consistent with the DSC results. The alloy with  $x=0.1$  that was annealed at 813 K for 180 s exhibits good soft magnetic properties, with  $H_c=12$  A/m and  $\mu_i=1.6 \times 10^4$ . For  $x=0.2$ , the optimal annealing temperature increases to 833 K, with  $H_c=33$  A/m and  $\mu_i=0.5 \times 10^4$ . Then, soft magnetic properties were deteriorated

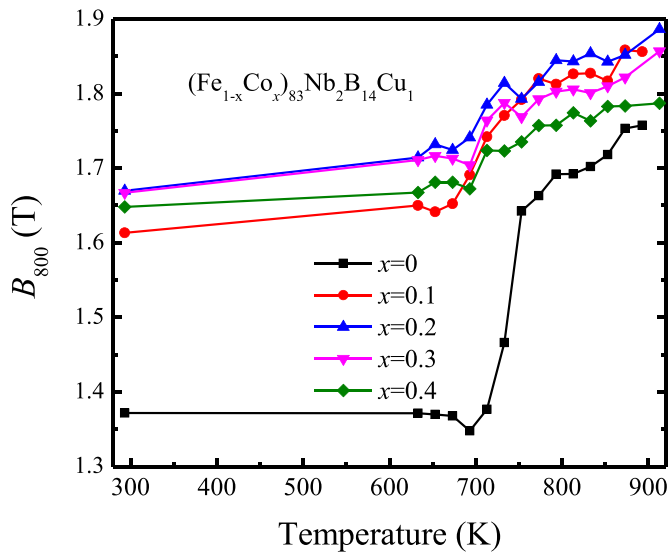


Fig. 3. Saturation magnetization versus  $T_a$  for annealed  $(\text{Fe}_{1-x}\text{Co}_x)_{83}\text{Nb}_2\text{B}_{14}\text{Cu}_1$  ( $x=0-0.4$ ) alloys.

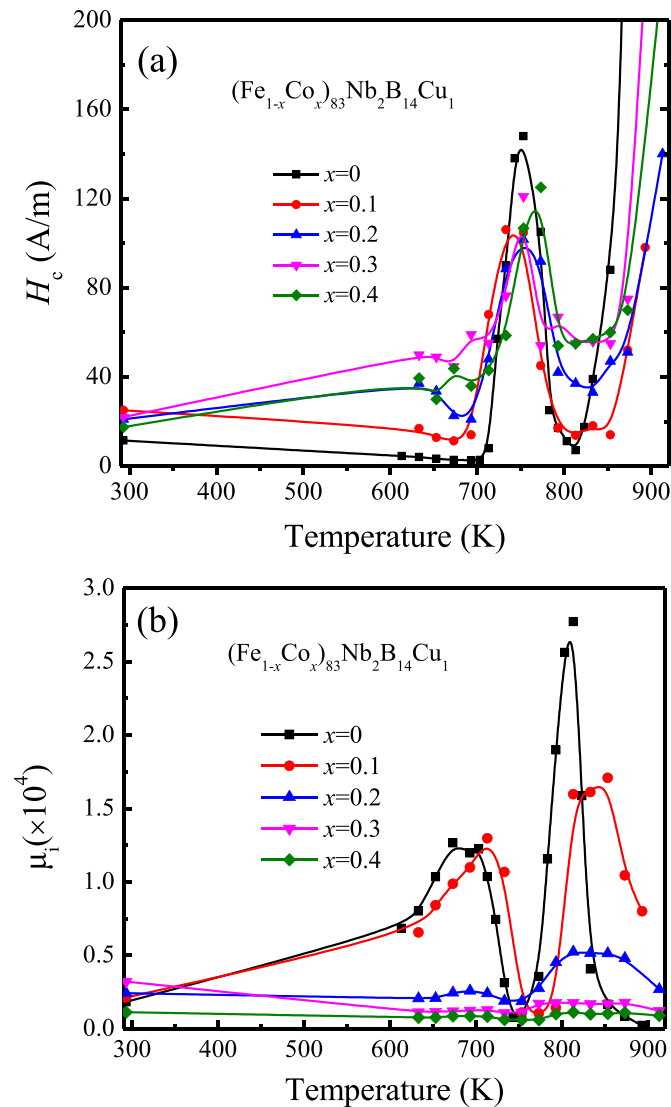


Fig. 4. Soft magnetic properties versus  $T_a$  for annealed  $(\text{Fe}_{1-x}\text{Co}_x)_{83}\text{Nb}_2\text{B}_{14}\text{Cu}_1$  ( $x=0-0.4$ ) alloys. (a) coercivity ( $H_c$ ), (b) initial permeability ( $\mu_i$ ). Lines for visual guidance.

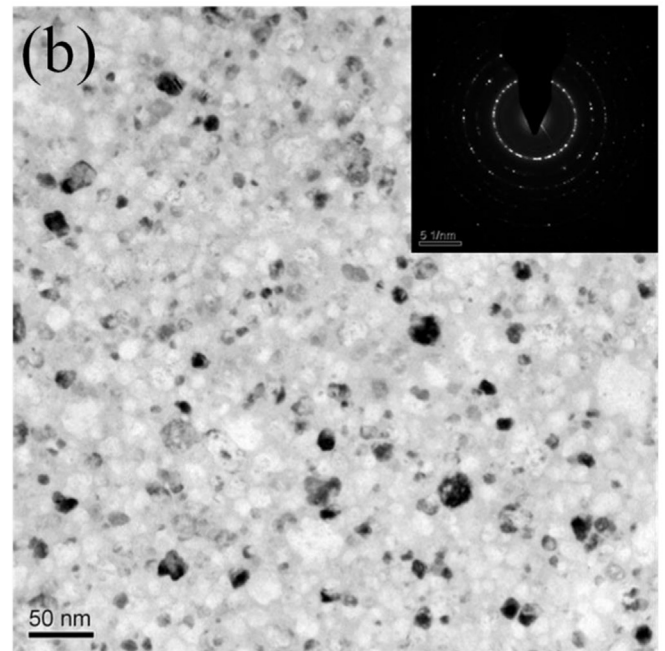
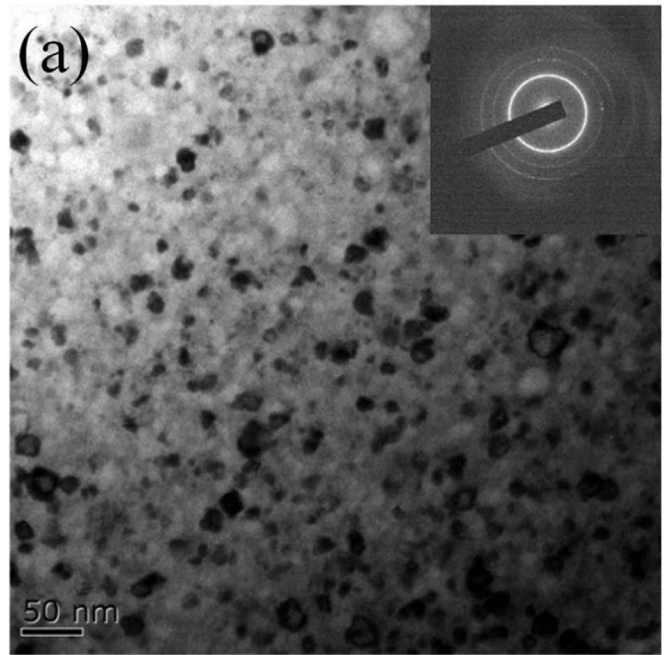


Fig. 5. Bright-field TEM, selected area diffraction pattern, and distribution of grain size of  $(\text{Fe}_{1-x}\text{Co}_x)_{83}\text{Nb}_2\text{B}_{14}\text{Cu}_1$  nanocrystalline alloys. (a)  $x=0.1$ ,  $T_a=813$  K, (b)  $x=0.2$ ,  $T_a=833$  K.

with further Co addition because of Co's large magneto-crystalline anisotropy; this is in accordance with the Slater–Pauling curves [26,27].

Nanocrystals that precipitated in the amorphous matrix between  $T_{x1}$  and  $T_{x2}$  were identified as  $\alpha$ -(Fe, Co) phase by XRD; grain sizes at different  $T_a$  were estimated from XRD patterns using Scherrer's equation. Furthermore, TEM was used to observe the microstructure of the  $(\text{Fe}_{0.9}\text{Co}_{0.1})_{83}\text{Nb}_2\text{B}_{14}\text{Cu}_1$  and  $(\text{Fe}_{0.8}\text{Co}_{0.2})_{83}\text{Nb}_2\text{B}_{14}\text{Cu}_1$  alloys annealed at 813 K and 833 K, respectively. Bright-field images and selected area electron diffraction (SAED) patterns are shown in Fig. 5. It can be seen from the bright-field TEM images that nanoscale grains precipitate randomly in the residual amorphous matrix. The SAED patterns also indicate that  $\alpha$ -(Fe, Co) nanocrystals oriented in the annealed samples randomly (inset in

Fig. 5(a) and (b)). At the optimum annealing temperature, microstructures with uniform and fine  $\alpha$ -(Fe, Co) grains were found, as shown in Fig. 5. Statistical analysis with respect to the grain size was carried out by analyzing more than 100 spots to seek a precise mean grain size. By careful determination of the grain size in the Gatan Digital Microscopy Suite, it was found that the mean grain size of the composites with  $\alpha$ -(Fe, Co) nanograins were 17 nm in Fig. 5(a) and 18 nm in Fig. 5(b). The results estimated from XRD are consistent with this; the grain size of Co-containing alloys are slightly larger than that of the base alloy [24].

From the above analysis, we can see that Co addition to the base alloy broadens the temperature intervals between the two crystallization temperatures ( $\Delta T_x = T_{x2} - T_{x1}$ ), favors the precipitation of  $\alpha$ -(Fe, Co), and inhibits the precipitation of other compounds. With minor Co addition ( $x=0.1$ ) and appropriate annealing conditions, the Fe–Co–Nb–B–Cu composite with refined  $\alpha$ -(Fe, Co) nanograins shows excellent magnetic properties with high  $B_{800}$  values above 1.82 T, a low coercivity of 12 A/m, and a high  $T_c$  above 1150 K, which is much higher than that of  $\text{Fe}_{83}\text{Nb}_2\text{B}_{14}\text{Cu}_1$ . Furthermore, a small quantity of Co did not coarsen the microstructure. The slight increase in  $H_c$  should be due to the large magneto-crystalline anisotropy constant of Co. Based on these findings, proper introduction of Co might be a good way to trigger nanocrystallization of  $\alpha$ -(Fe, Co), averaging out the magnetic anisotropy and therefore enhancing the soft magnetic properties.

#### 4. Conclusions

In this work, the microstructures and soft magnetic properties of  $(\text{Fe}_{1-x}\text{Co}_x)_{83}\text{Nb}_2\text{B}_{14}\text{Cu}_1$  with small amounts of Co were investigated, the main results of which can be summarized as follows:

- (1) Co addition broadens the temperature interval between the two crystallization temperatures ( $\Delta T_x = T_{x2} - T_{x1}$ ), favors the precipitation of  $\alpha$ -(Fe, Co), inhibits the precipitation of other compounds, and increases  $T_c$  to above 1150 K.
- (2) With the introduction of a little Co and appropriate annealing conditions, Fe–Co–Nb–B–Cu nanocrystalline alloys show uniform microstructures and exhibit high saturation magnetic flux density (1.82 T), and low coercivity (12 A/m).

#### Acknowledgments

This work was supported by the National Natural Science Foundation of China (Grant nos. 51401052, 51271194 and 51471050) and the Fundamental Research Funds for the Central Universities (No. 3212006702).

#### References

- [1] P. Duwez, S.C.H. Lin, Amorphous ferromagnetic phase in iron-carbon-phosphorus alloys, *J. Appl. Phys.* 38 (10) (1967) 4096–4097.
- [2] M.E. McHenry, M.A. Willard, D.E. Laughlin, Amorphous and nanocrystalline materials for applications as soft magnets, *Progress Mater. Sci.* 44 (4) (1999) 291–433.
- [3] R. Hasegawa, Advances in amorphous and nanocrystalline materials, *J. Magn. Magn. Mater.* 324 (21) (2012) 3555–3557.
- [4] Y. Naitoh, T. Bitoh, T. Hatanai, et al., Application of nanocrystalline soft magnetic Fe–M–B (M=Zr, Nb) alloys to choke coils, *J. Appl. Phys.* 83 (11) (1998) 6332–6334.
- [5] W.H. Wang, C. Dong, C.H. Shek, Bulk metallic glasses, *Mater. Sci. Eng. R Rep.* 44 (2–3) (2004) 45–89.
- [6] J. Torrens-Serra, M. Stoica, J. Bednarcik, et al., Elastic and anelastic properties close to the Curie temperature of Fe-based bulk metallic glass, *Appl. Phys. Lett.* 102 (4) (2013) 041904.
- [7] C.C. Dun, H.S. Liu, L. Hou, et al., Ductile Co–Nb–B bulk metallic glass with ultrahigh strength, *J. Non-Cryst. Solids* 386 (2014) 121–123.
- [8] Z.Z. Li, S.X. Zhou, R. Xiang, et al., The corrosion resistance of FeSiBPNCu bulk metallic glasses in sulphuric acid solutions, *Mater. Res. Innov.* 19 (2015) S333–S336.
- [9] K. Suzuki, J.M. Cadogan, Random magnetocrystalline anisotropy in two-phase nanocrystalline systems, *Phys. Rev. B* 58 (5) (1998) 2730–2739.
- [10] G. Herzer, Modern soft magnets: amorphous and nanocrystalline materials, *Acta Mater.* 61 (3) (2013) 718–734.
- [11] W.M. Yang, H.S. Liu, L. Xue, et al., Magnetic properties of  $(\text{Fe}_{1-x}\text{Ni}_x)_{72}\text{B}_{20}\text{Si}_4\text{Nb}_4$  ( $x=0.0-0.5$ ) bulk metallic glasses, *J. Magn. Magn. Mater.* 335 (0) (2013) 172–176.
- [12] X.D. Fan, H. Men, A.B. Ma, et al., Soft magnetic properties in  $\text{Fe}_{84-x}\text{B}_{10}\text{C}_6\text{Cu}_x$  nanocrystalline alloys, *J. Magn. Magn. Mater.* 326 (2013) 22–27.
- [13] Y. Yoshizawa, S. Oguma, K. Yamauchi, New Fe-based soft magnetic alloys composed of ultrafine grain structure, *J. Appl. Phys.* 64 (10) (1988) 6044–6046.
- [14] K. Suzuki, A. Inoue, Soft magnetic properties of bcc Fe–MB–Cu (M=Ti, Nb or Ta) alloys with nanoscale grain size, *Jpn. J. Appl. Phys.* 30 (part 2) (1991).
- [15] M.A. Willard, D.E. Laughlin, M.E. McHenry, et al., Structure and magnetic properties of  $(\text{Fe}_{0.5}\text{Co}_{0.5})_{88}\text{Zr}_7\text{B}_4\text{Cu}_1$  nanocrystalline alloys, *J. Appl. Phys.* 84 (12) (1998) 6773–6777.
- [16] J.S. Blázquez, V. Franco, C.F. Conde, et al., Microstructure and magnetic properties of  $\text{Fe}_{78-x}\text{Co}_x\text{Nb}_6\text{B}_{15}\text{Cu}_1$  ( $x=18, 39, 60$ ) alloys, *J. Magn. Magn. Mater.* 254 (2003) 460–462.
- [17] R. Xiang, S.X. Zhou, B.S. Dong, et al., Effect of Co addition on crystallization and magnetic properties of FeSiBPCu alloy, *Progress Nat. Sci. Mater. Int.* 24 (6) (2014) 649–654.
- [18] Y. Zhang, P. Sharma, A. Makino, Effects of Cobalt Addition in Nanocrystalline Soft Magnetic Alloy, *Magn.*, *IEEE Trans.* 50 (4) (2014) 1–4.
- [19] M.X. Zhang, J.W. Li, F.L. Kong, et al., Magnetic properties and magnetocaloric effect of FeCrNbYB metallic glasses with high glass-forming ability, *Intermetallics* 59 (2015) 18–22.
- [20] L.F. Kiss, T. Kemény, V. Feanco, et al., Enhancement of magnetocaloric effect in B-rich FeZrBCu amorphous alloys, *J. Alloy. Compd.* 622 (2015) 756–760.
- [21] R. Caballero-Flores, V. Franco, A. Conde, et al., Influence of Co and Ni addition on the magnetocaloric effect in  $\text{Fe}_{88-2x}\text{Co}_x\text{Ni}_x\text{Zr}_7\text{B}_4\text{Cu}_1$  soft magnetic amorphous alloys, *Appl. Phys. Lett.* 96 (18) (2010) 182506.
- [22] V. Franco, J.S. Blázquez, M. Millán, et al., The magnetocaloric effect in soft magnetic amorphous alloys, *J. Appl. Phys.* 101 (2007) 09C503.
- [23] V. Franco, J.S. Blázquez, A. Conde, The influence of Co addition on the magnetocaloric effect of Nanoperm-type amorphous alloys, *J. Appl. Phys.* 100 (6) (2006) 064307.
- [24] L. Xue, H.S. Liu, L.T. Dou, et al., Soft magnetic properties and microstructure of  $\text{Fe}_{84-x}\text{Nb}_2\text{B}_{14}\text{Cu}_x$  nanocrystalline alloys, *Mater. Des.* 56 (2014) 227–231.
- [25] R. Victora, L. Falicov, Calculated magnetization of iron-cobalt disordered alloys, *Phys. Rev. B* 30 (1) (1984) 259–262.
- [26] J.C. Slater, Electronic structure of alloys, *J. Appl. Phys.* 8 (6) (1937) 385–390.
- [27] L. Pauling, The nature of the interatomic forces in metals, *Phys. Rev.* 54 (11) (1938) 899.